

Study of Meltblown Structures Formed By Robotic and Meltblowing Integrated System: Impact of Process Parameters On Fiber Diameter Distributions

By Raoul Farer, Subhash K. Batra, Tushar K. Ghosh, Eddie Grant¹ and Abdelfattah M. Seyam, College of Textiles, North Carolina State University, Raleigh, NC 27695 USA

In previous publication, the influence of process parameters on the fiber orientation of the meltblown web was evaluated [4]. The meltblown webs were formed using Robotic Fiber Assembly and Control System (RFACS), which is described in previous publications [3, 4]. In this paper, parametric studies evaluating the effect of polymer throughput rate, attenuating air pressure and temperature, and die temperature, on fiber diameter distributions of meltblown webs from polypropylene produced by RFACS are reported. Fiber diameters were determined by analyzing fabric images obtained through scanning electron microscopy (SEM). Under the specific conditions explored, the fraction of fibers of diameter smaller than 10 microns (μm) can increase by 72% with a 7.9×10^{-2} g/min/hole (82%) reduction in throughput. A 54% increase of the same can be observed with a 2.8 bar (400%) increase in attenuating air pressure. A change of 45°C (16 %) in air temperature is shown not to significantly affect fiber diameters produced, while an increase of 67°C (26%) in die temperatures can result in an increase of 17% in the fraction of fibers of diameter smaller than 10 μm . All fiber diameter distributions are shown to be unique to the condition evaluated as no overlap across distributions for changes in a given parameter is observed. Further fiber fraction smaller than 10 μm data is also shown to be unique to each parameter evaluated.

Key Words

Meltblowing, Robot, Orientation Distribution Function (ODF), Approach Angle, die-to-collector-distance, three-dimension (3D), 3D Mold, take-up speed, Die Temperature, polymer throughput, attenuating air pressure, attenuating air temperature, Die Temperature, Image Analysis, SEM, Fiber Diameter, Fiber Diameter Distribution, Polypropylene.

Introduction

It is well known that while a meltblowing process produces finer fibers relative to conventional fiber spinning processes, the distributions of fiber diameter are usually quite broad. Because lower mean values and narrower distributions lead to smaller pore sizes (lower mean and narrow distributions) and higher surface area, the control of fiber diameter distribution is considered highly desirable [14], for a number of important applications.

Average fiber diameter data for meltblown webs has been previously available in the literature, and is incorporated, here, for purposes of comparison and analysis of the observed fiber diameter distributions. Review of the literature suggests that final fiber diameter is formed within 6 cm of the die orifice exit [1]. Die-to-collector distance (DCD) used in this study was held constant at either 14 or 18 cm, and the angle of approach (defined in previous publication [4]) maintained at 90° to the collector drum surface.

1. College of Engineering, NC State University

Experimental

Material and Methods

Nonwoven meltblown samples were produced using Polypropylene PP resin with nominal 1200 melt-flow-rate (MFR) (IV: 0.8) on a small, 7.8 cm (3 inch) slot-die melt-blowing unit. The equipment specifications were given elsewhere [4]. For the study reported here, the fabrics were formed onto a 21 cm diameter collector drum.

All samples were prepared using a normal, 90° vertical fiber approach angle to the horizontal drum collector. The effects of gravity were therefore acting along the fiber stream path. This eliminated gravity as a variable in the study. Through use of the collector drum, followed by a separate winding capability, continuous, approximately 8 cm wide, samples were obtained. SEM images were taken for individual samples (1 cm x 1 cm) for each fabric type. All samples were placed face down on a sample holder.

Fiber Diameter Measurement

For most samples, SEM images were obtained at 600X and subsequently measuring more than 20 fiber images observed in each case. Some samples required lower or higher magnification (400X, 2000X). Fiber diameters were measured using an image analysis package developed by Dr. Pourdeyhimi at the Nonwovens Cooperative Research Center. A well-developed protocol for adjusting the SEM image (*Figure 2*) was followed before a final black and white fiber image (*Figure 1*) was evaluated for fiber diameters. The procedure followed in the image analysis software measures the distribution of fiber diameters by finding the central medial axis along each fiber axis. At every pixel along the central medial axis certain intensity relative to the distance from the edges of the fiber image is assigned. The observed intensities are representative of the fiber diameter and are subsequently used to calculate the overall distribution [9].

For a fabric corresponding to a given set of processing conditions, typically four samples taken randomly along the length of the roll, were evaluated. Each sample was evaluated in two locations. The frequency distribution data so obtained were averaged to obtain a representative distribution. Cumulative frequency distributions of fiber diameters were evaluated, and representative standard error values of the distributions are reported in some of the figures.

Processing Parameters

A wide range of fabric samples was formed employing a variety of processing conditions. These were:

Polymer Throughput Rates: 1.7, 3.7, 5.4, 8.1, and 9.6×10^2 g/min/hole.

Attenuating Air Pressures: 0.7, 1.4, 2.1, 2.8, and 3.5 bar.

Attenuating Air Temperatures: 282°C, 304°C, and 327°C.

Die Temperatures: 260°C, 293 °C, and 327°C.

Constant Parameters: (1) DCD = 14 or 18 cm, (2) take-up speed = 15 or 21 m/min, (3) Extruder Temperatures in Zones 1-3: 160°C, 193°C, 232°C.



Figure 1
FIBER IMAGE USED FOR FIBER
DIAMETER ANALYSIS

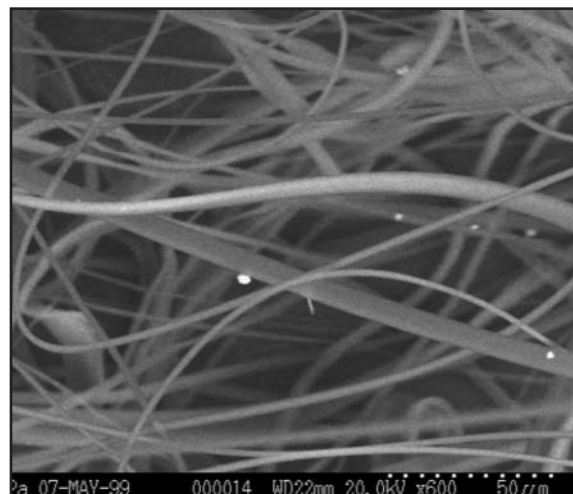


Figure 2
A TYPICAL SEM IMAGE (FABRIC DP5)

Results and Discussion

The results showing influences of different process parameters are given in figures showing cumulative frequency distributions of fiber diameters. The “fraction of fibers smaller than 10 μ m in diameter” was chosen as a metric of the influence, since production of fine fibers is a dominant goal in meltblowing.

Influence of Polymer Throughput Rate and Attenuating Air Pressure

Figure 3 shows cumulative frequencies of fiber diameter distributions of PP meltblown fabrics formed at different levels of polymer throughput rates and at a selected level of attenuating air pressure. *Figure 4* shows cumulative frequencies of fiber diameters in fabrics produced at varying attenuating air pressure and a selected polymer throughput rate. *Figure 2* shows a SEM image of a typical fabric (produced at 9.6×10^2 g/min/hole, 3.5 bar air pressure, 282°C air temp. and 260°C die temp. settings)

All fabric samples in *Figure 3* show fiber diameters to decrease and their distribution to narrow with a decrease in

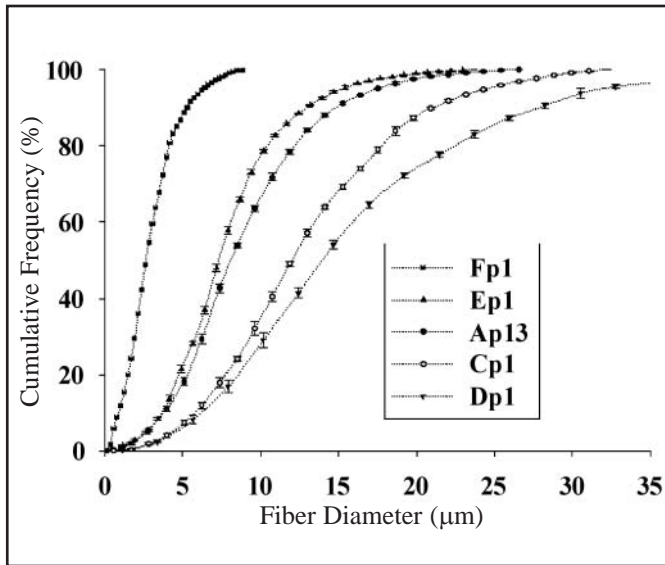


Figure 3

CUMULATIVE FREQUENCY DISTRIBUTION OF FIBER DIAMETERS AT DIFFERENT POLYMER THROUGHPUT RATES; 0.7 BAR AIR PRESSURE, 282 °C AIR TEMP., AND 260 °C DIE TEMP.; Fp1: 1.7×10^{-2} G/MIN HOLE; Ep1: 3.7×10^{-2} G/MIN/HOLE; Ap13: 5.4×10^{-2} G/MIN/HOLE; Cp1: 8.1×10^{-2} G/MIN/HOLE; AND Dp1: 9.6×10^{-2} G/MIN/HOLE

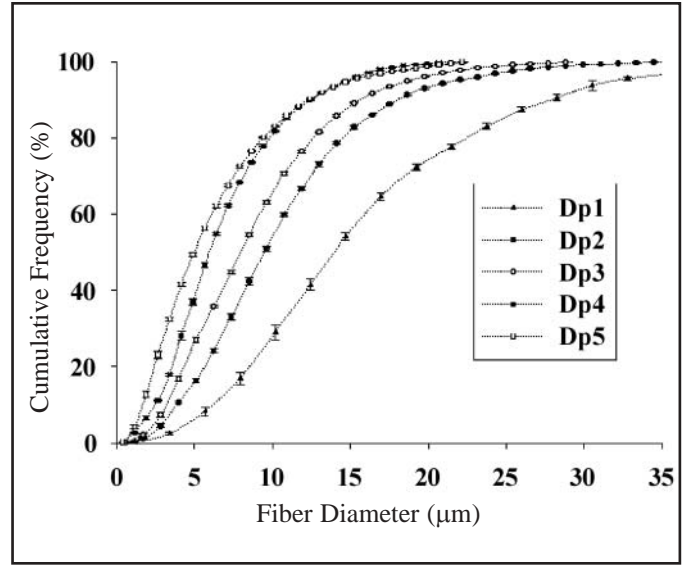


Figure 4

CUMULATIVE FREQUENCY DISTRIBUTION OF FIBER DIAMETERS AT DIFFERENT ATTENUATING AIR PRESSURES; 9.6×10^{-2} G/MIN/HOLE THROUGHPUT RATE, 282 °C AIR TEMP., AND 260 °C DIE TEMP.; Dp1: 0.7 BAR; Dp2: 1.4 BAR; Dp3: 2.1 BAR; Dp4: 2.8 BAR; AND Dp5: 3.5 BAR

throughput rate. Fiber diameter distributions for various throughput rates shown do not overlap and decreases are shown to be successive according to polymer throughput rates employed. *Figure 4* shows cumulative frequencies for fiber diameter distributions in fabrics formed at varying attenuating air pressures, but a constant polymer throughput rate of 9.6×10^{-2} g/min/hole, and the same temperature settings as in *Figure 3*. Fiber diameters decrease with increase in attenuating air pressures in all cases; broader distributions of fiber diameters are observed with decreases in attenuating air pressures.

Figure 5 shows fraction of fibers smaller than $10\mu\text{m}$ in diameter for fabric samples formed at varying polymer throughput rates and attenuating air pressures. All samples depict the same trend of increasing fraction of small diameter fibers with decreasing throughput rates; the increase in attenuating air pressure also increases the fraction of fine (less than $10\mu\text{m}$) fibers. The most rapid increase in fraction of fine fibers with a decrease in polymer throughput rates, 28.17% to 100%, is observed at attenuating air pressures of 0.7 bar. With increasing attenuating air pressure the fraction of smaller than $10\mu\text{m}$ fibers increases for a fixed throughput rate. Indeed, there appears to be a processing envelope outside of which (higher attenuating air pressure, lower throughput rate) it is difficult to form and collect a fabric.

In the same vein *Figure 6* shows fraction of fibers smaller than $10\mu\text{m}$ produced at different attenuating air pressure and throughput rate. All samples show the same trend of increasing

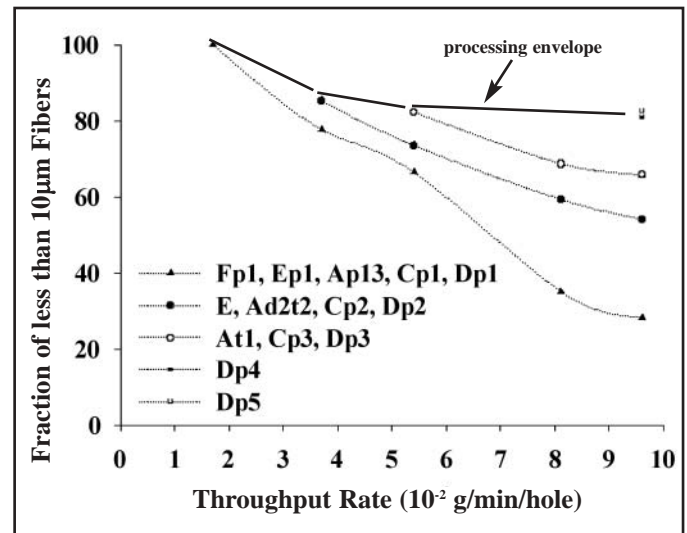


Figure 5

INFLUENCE OF POLYMER THROUGHPUT RATES AND ATTENUATING AIR PRESSURES ON FRACTION OF FIBERS SMALLER THAN $10 \mu\text{m}$ AT 282 °C AIR TEMP., AND 260 °C DIE TEMP; Fp1, Ep1, Ap13, Cp1, AND Dp1: 0.7 BAR; E, Ad2t2, Cp2, AND Dp2: 1.4 BAR; At1, Cp3, AND Dp3: 2.1 BAR; Dp4: 2.8 BAR; AND Dp5: 3.5 BAR

fraction of small diameter fibers with increases in attenuating air pressures. Lowest throughput rate and lowest attenuating air pressure appear to provide the highest percentage of fine fibers.

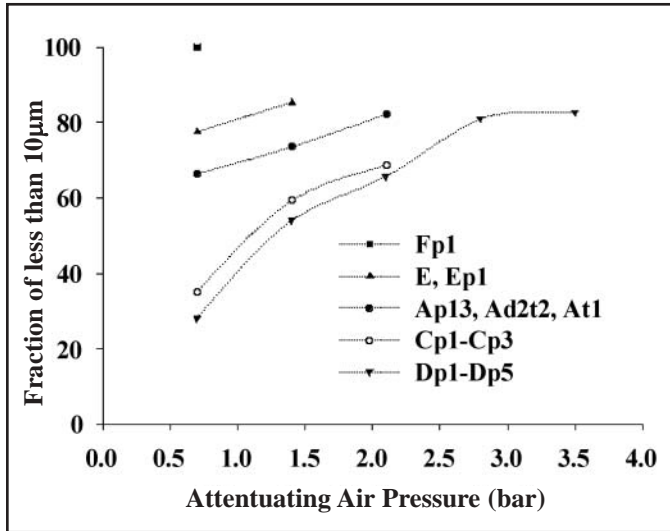


Figure 6

INFLUENCE OF ATTENUATING AIR PRESSURES AND POLYMER THROUGHPUT RATES ON FRACTION OF FIBERS SMALLER THAN 10 μM AT 282 °C AIR TEMP., AND 260 °C DIE TEMP; Fp1: 1.7×10^{-2} G/MIN/HOLE THROUGHPUT RATE; E, Ep1: 3.7×10^{-2} G/MIN/HOLE THROUGHPUT RATE; Ap13, Ad2t2, At1: 5.4×10^{-2} G/MIN/HOLE THROUGHPUT RATE; Cp1-Cp3: 8.1×10^{-2} G/MIN/HOLE THROUGHPUT RATE; AND Dp1-Dp5: 9.6×10^{-2} G/MIN/HOLE THROUGHPUT RATE

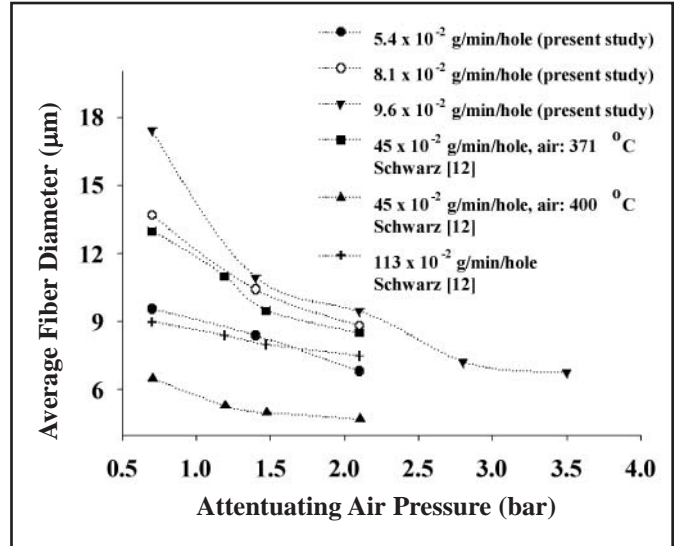


Figure 8

COMPARISON OF AVERAGE FIBER DIAMETER AS A FUNCTION OF ATTENUATING AIR PRESSURE

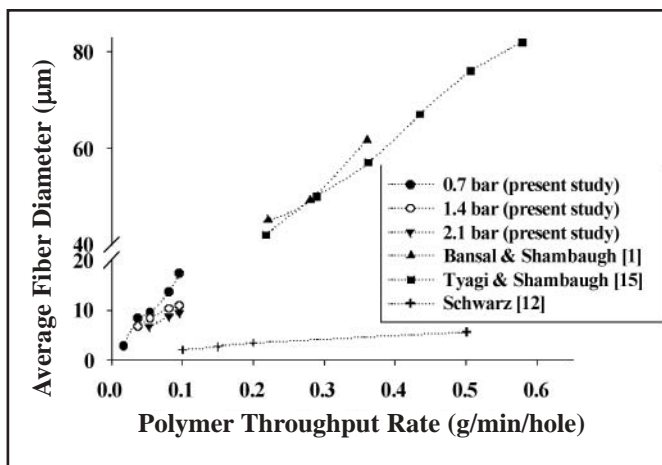


Figure 7

COMPARISON OF AVERAGE FIBER DIAMETER AS A FUNCTION OF POLYMER THROUGHPUT RATES

An increase in attenuating air pressure results in higher velocity of forming air, exerting higher drag forces on the polymer mass as it is being drawn out of the die orifices, as well as resulting in higher fiber velocities [1, 16]. Higher drag apparently attenuates the polymer mass to finer diameters, analogous to higher take-up roller speeds resulting in finer

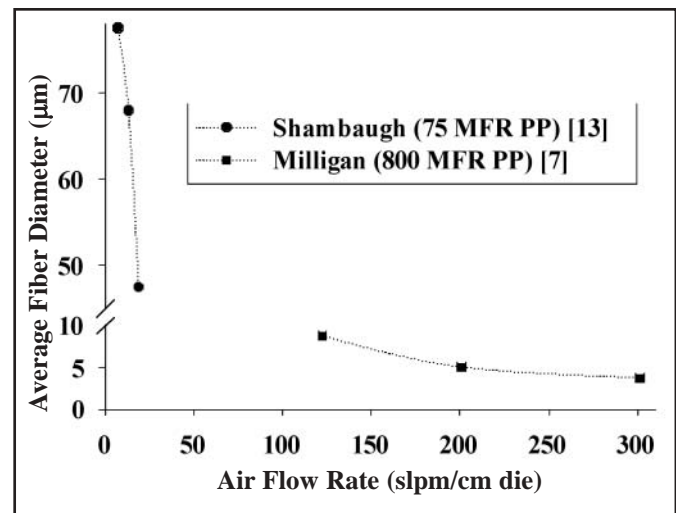


Figure 9

COMPARISON OF PREVIOUS INVESTIGATION ON AVERAGE FIBER DIAMETER AND AIR FLOW RATE

diameter filaments in conventional spinning. *Figure 6* gives a comprehensive view of this effect over a range of throughput rates. In the cases studied the fraction of fibers less than 10 μm can increase by 54% at a polymer throughput rate of 9.6×10^{-2} g/min/hole. Similar trends are observed for the other throughput rates investigated.

Somewhat similar observations have been reported in previous studies. For example, increasing average fiber diameter with increasing polymer throughput rates has been reported [1, 2, 8, 12, 14, 15]. *Figure 7* compares some previous data with those obtained in the present study.

While the trend of increasing average fiber diameter with increasing throughput rate is evident in all cases, the present

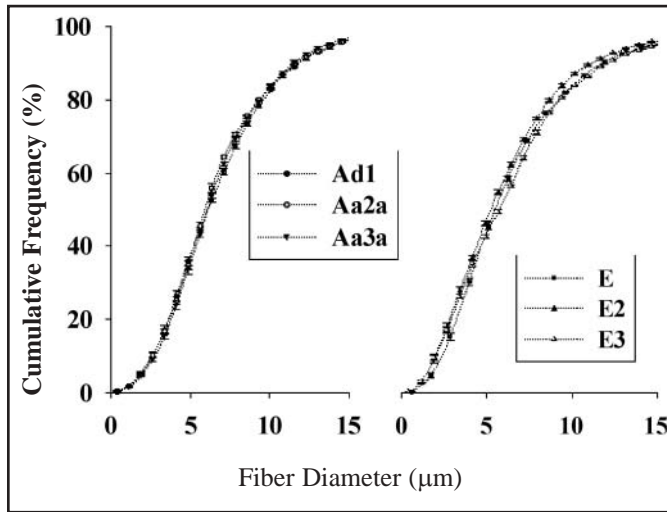


Figure 10

CUMULATIVE FREQUENCY DISTRIBUTION OF FIBER DIAMETERS AT DIFFERENT ATTENUATING AIR TEMPERATURES; 5.4×10^{-2} G/MIN/HOLE THROUGHPUT RATE, 1.4 BAR ATTENUATING AIR PRESSURE, AND 260 °C DIE TEMP.: Ad1: 282 °C, Aa2a: 305 °C, AND Aa3a: 327 °C; 3.7×10^{-2} G/MIN/HOLE THROUGHPUT RATE, 1.4 BAR ATTENUATING AIR PRESSURE, AND 260 °C DIE TEMP.: E: 282 °C, E2: 304 °C, AND E3: 327 °C

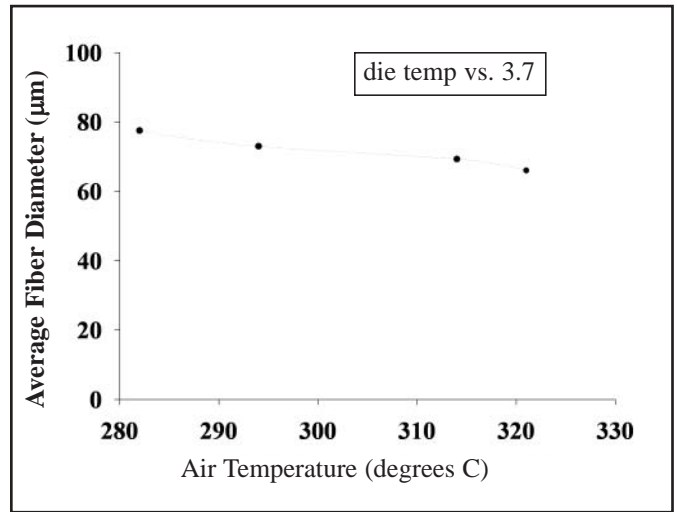


Figure 12

AVERAGE FIBER DIAMETER VARYING ATTENUATING AIR TEMPERATURE AS DETERMINED BY SHAMBAUGH [14]; POLYMER TEMPERATURE 350°C

the starting resin. The MFR value for Bansal, Tyagi, and Shambaugh [1, 15] was 75, for Schwarz [12] 35, and for the present study 1200.

In the same vein the influence of forming air velocity (or attenuating air pressure) on fiber diameter has been studied previously [2, 6, 7, 12, 13, 15]. An increase in attenuating air pressures, synonymous to an increase in airflow rate, are shown to result in significant reduction in fiber diameter (*Figures 8 and 9*). Air pressure data in Schwarz's patent [12], see *Figure 8*, is comparable in trend and magnitude to the average fiber diameter data obtained in this study.

Influence of Attenuating Air Temperature

Figure 10 shows cumulative frequencies for fiber diameter distributions obtained using varying attenuating air temperature. Fiber diameter was hardly affected by the attenuating air temperature in the range of (282°C – 327°C) studied.

Similar trends were observed in a study by Rao and Shambaugh, where a 100°C increase in air temperature did not show much effect on fiber diameter [10]. In both Rao and Shambaugh and our case discussed, the polymer (die temperature) settings were lower than the attenuating air temperature. In *Figure 11*, the observed air temperature profile, measured by a handheld thermocouple at the die-orifice exit, is given for the conditions evaluated. In another study by Shambaugh [14], when the die temperature was higher than the attenuating air temperatures employed, reductions in fiber diameter were observed with increases in air temperature, see *Figure 12*. As is evident from the observed temperature profile, actual air temperatures do change significantly, even when the employed die temperature is lower than the air temperature. It is observed that the attenuating air temperatures studied in this research were not high enough to significantly cause changes in diameters of the meltblown fibers formed.

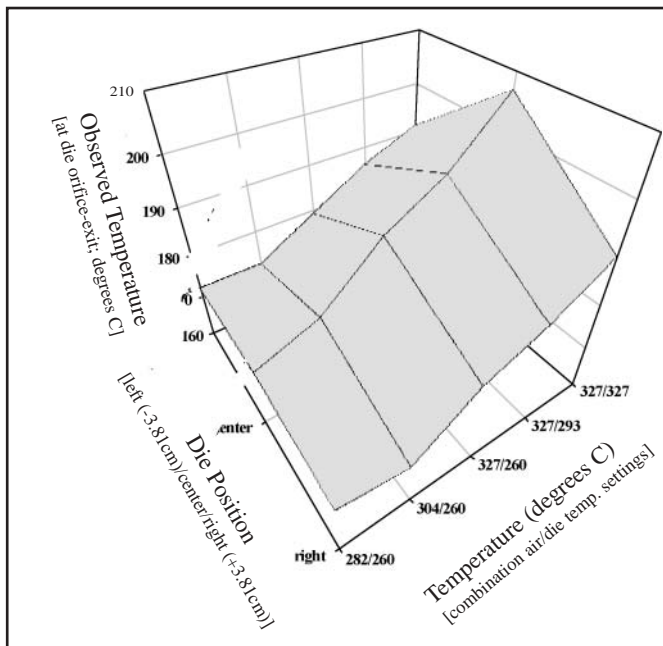


Figure 11

OBSERVED TEMPERATURE PROFILE AT DIE ORIFICE EXIT

study covers significantly lower throughput rates and obtains significantly finer fiber. It is worthy of note that the fiber diameters are also governed by molecular weight structure of

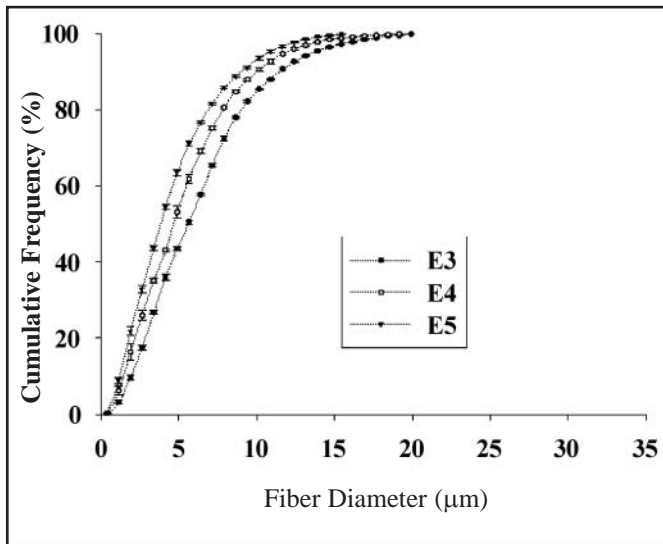


Figure 13

CUMULATIVE FREQUENCY DISTRIBUTION OF FIBER DIAMETERS AT DIFFERENT DIE TEMPERATURE; 3.7×10^{-2} G/MIN/HOLE POLYMER THROUGHPUT RATE; 1.4 BAR ATTENUATING AIR PRESSURE, AND 327 °C ATTENUATING AIR TEMP.; E3: 260 °C; E4: 293 °C; AND E5: 327 °C DIE TEMPERATURE

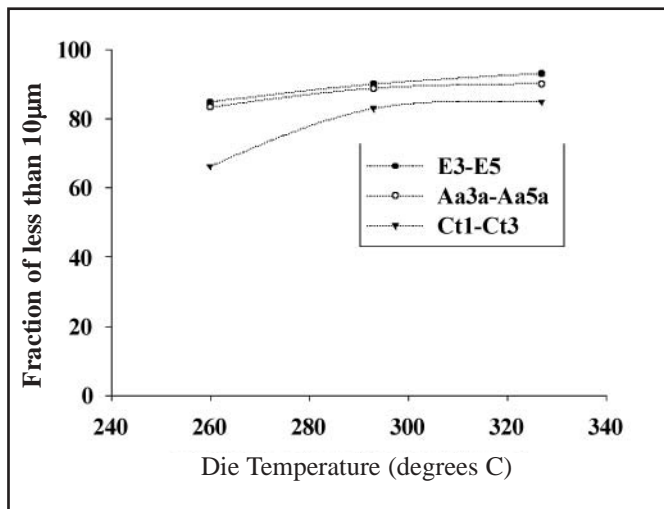


Figure 14

INFLUENCE OF DIE TEMPERATURE ON FRACTION OF FIBERS SMALLER THAN 10 μM AT 327 °C AIR TEMP.; E3-E5: 3.7×10^{-2} G/MIN/HOLE POLYMER THROUGHPUT RATE, AND 1.4 BAR ATTENUATING AIR PRESSURE; Aa3a-Aa5a: 5.4×10^{-2} G/MIN/HOLE POLYMER THROUGHPUT RATE, AND 1.4 BAR ATTENUATING AIR PRESSURE; AND Ct1-Ct3: 8.1×10^{-2} G/MIN/HOLE POLYMER THROUGHPUT RATE, AND 2.1 BAR ATTENUATING AIR PRESSURE

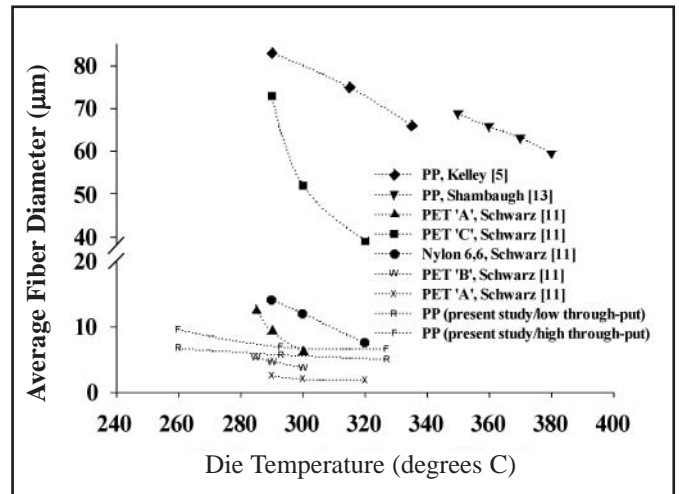


Figure 15

COMPARISON OF AVERAGE FIBER DIAMETER AS A FUNCTION OF DIE TEMPERATURE

Influence of Die Temperature

Figure 13 shows cumulative frequencies for fiber diameter distributions of PP meltblown fabrics formed due to varying die temperatures. As is apparent, fiber diameter decreased with increases in die temperature.

Figure 14 shows fraction of fibers smaller than 10 μm in diameter for fabric samples formed due to varying die temperatures and at different throughput rates. All samples show increases in fine fiber content with increasing die temperature.

The dominant resultant effect of an increase in die temperature is lower polymer viscosity in the die body. A lower viscosity liquid will show less physical resistance to high velocity attenuating air, and allow finer fiber diameters to form. The reduction in polymer viscosity appears to be more significant over the temperature range evaluated, as similar changes in air temperatures have in this study not been able to show a lasting effect. Reduction in polymer viscosity would further show a larger effect at higher polymer throughput rates, where finer diameter fibers are formed with more difficulty. Figure 14 shows this effect to be true, as larger increases in fraction of fine fiber diameter are initially apparent at higher throughput rates (Ct1-Ct3).

Decreases in fiber diameter with increases in die temperature were also observed by other researchers, see Figure 15, [1, 5, 11, 13]. Data shown in Figure 15 for PET 'A', as triangle pointing up, was produced at a higher polymer throughput rate than data for PET 'A' depicted with an 'X.' This undermines our earlier statement of reduction in polymer viscosity to show a more significant effect at higher polymer throughput. Clearly, PET data shown by a triangle exhibit a larger reduction in fiber diameter with increasing die temperature, than PET data shown by an 'X.'

Conclusion

Fiber diameter distributions were shown to correlate well to processing conditions employed in meltblowing of

polypropylene resin. Fiber diameters were demonstrated to reduce with reductions in throughput rate, and increases in attenuating air pressures and die temperatures. Air temperatures in the range studied, below 210°C at the die-orifice exit, were shown to not affect fiber diameter distributions. Good agreement for all results was also found to average fiber diameter data observed in published literature.

Acknowledgements

This research was supported in part by an ARO-MURI grant from the Army Research Office, and in part by support from the Nonwovens Cooperative Research Center, North Carolina State University. We gratefully acknowledge their generous support of this project.

References

1. Bansal, Vishal, Robert L. Shambaugh, On-line Determination of Diameter and Temperature during Melt Blowing of Polypropylene, *Ind. Eng. Chem. Res.*, 37, 1799-1806 (1998).
2. Butin, Robert R., J. P. Keller, J. W. Harding, Non-Woven Mats by Melt Blowing, U.S. Patent 3,849,241, Nov. 19th, 1974.
3. Farer, R., Formation of 3D Meltblown Structures Using Robotic Control of Fiber Deposition, Ph.D. Thesis, NC State University, 1999.
4. Farer, R., Ghosh, T. K., Seyam, A. M., Grant, E., and Batra, S. K., Study of Meltblown Structures Formed by Robotic and Meltblowing Integrated System: Impact of Process Parameters on Fiber Orientation, *Int'l Nonwovens Journal*, 11 No. 4 (2002).
5. Kelley, Stephen L., R. L. Shambaugh, Sheath-Core Differences Caused by Rapid Thermo-oxidation during Melt Blowing of Fibers, *Ind. Eng. Chem. Res.* 37, 1140-1153 (1998).
6. Milligan, M. W., F. Utsman, An Investigation of the Meltblown Web Defect Known as Shot, *Int'l Nonwovens Journal*, 7, 65-68 (1995).
7. Milligan, M. W., R. R. Buntin, F. Lu, Method and Apparatus for Treating Meltblown Filaments, U.S. Patent 5,075,068, Dec. 24th, 1991.
8. Nyssen, Peter R., W. Wagner. D. Birkenhaus, Method and Device for Manufacturing Ultrafine Fibers from Thermoplastic Polymers, US Patent 5,260,003, Nov. 9th, 1993.
9. Pourdeyhimi, B., Online 'Image' Product Literature, Barn Engineering, Roswell, GA, 1998.
10. Rao, Rajiv. S, R. L. Shambaugh, Vibration and Stability in the Melt Blowing Process, *Ind. Eng. Chem. Res.* 32, 3100-3111 (1993).
11. Schwarz, E. C., Process for Forming Non-Woven Webs from highly Oriented Melt Blown Fibers, U.S. Patent 4,731,215, Mar. 15th, 1988.
12. Schwarz, E. C., Apparatus and Process for Melt-Blowing a Fiberforming Thermoplastic Polymer and Product Produced Thereby, U.S. Patent 4,380,570, April 19th, 1983.
13. Shambaugh, R. L., Modeling of the Next Generation of

Melt-Blowing – Part II, Tappi Nonwovens Conference, 43-49, 1996.

14. Shambaugh, Robert, A Macroscopic View of the Melt-Blowing Process for Producing Microfibers, *Ind. Eng. Chem. Res.*, 27, 2363-2372 (1988).

15. Tyagi, Manoj K., R. S. Shambaugh, Use of Oscillating Gas Jets in Fiber Processing, *Ind. Eng. Chem. Res.*, 34, 656-660 (1995).

16. Uyttendale, Marc A. J., R. L. Shambaugh, Melt Blowing: General Equation Development and Experimental Verification, *AIChE Journal*. 36, 175-186 (1990). — *INJ*